



Structural and thermal analyses of zinc and lactose in homeopathic triturated systems

Carla Holandino^{1,*}, Adriana Passos Oliveira¹, Fortune Homsani¹, Juliana Patrão de Paiva¹, Gleyce Moreno Barbosa¹, Michelle Rodrigues de Lima Zanetti¹, Thaís de Barros Fernandes¹, Camila Monteiro Siqueira^{1,2}, Venicio Feo da Veiga³, Letícia Coli Louvise de Abreu⁴, Marta Marzotto⁵, Paolo Bernardi⁶, Leoni Villano Bonamin⁷, Paolo Bellavite⁵, André Linhares Rossi⁸ and Paulo Henrique de Souza Picciani⁹

¹Multidisciplinary Laboratory of Pharmaceutical Sciences and Laboratory of Research and Development of Integrative and Complementary Medicine, Department of Drugs and Medicines, Pharmacy College, UFRJ, Rio de Janeiro, Brazil

²Federal Institute of Rio de Janeiro, Brazil

³Laboratory of Electron Microscopy, Institute of Microbiology Prof. Paulo de Góes IMPPG, UFRJ, Rio de Janeiro, Brazil

⁴Laboratory of Pharmaceutical Technology, LabTIF, Department of Drugs and Medicines, Pharmacy College, UFRJ, Rio de Janeiro, Brazil

⁵Department of Medicine, General Pathology Section, University of Verona, Italy

⁶Department of Neurosciences, Biomedicine and Movement Sciences, Anatomy and Histology Section, University of Verona, Italy

⁷Research Center, Paulista University, São Paulo, SP, Brazil

⁸Department of Applied Physics, Brazilian Center for Research in Physics, Urca, Rio de Janeiro, RJ, Brazil

⁹Institute of Macromolecules Professor Eloisa Mano, Federal University of Rio de Janeiro, Rio de Janeiro, RJ, Brazil

Background: A series of different experimental approaches was applied in *Zincum metallicum* (*Zinc met.*) samples and lactose controls. Experiments were designed to elucidate the effect of zinc trituration and dynamization on physicochemical properties of homeopathic formulations, using lactose as excipient.

Methods: *Zinc met.* potencies (*Zinc met* 1–3c) were triturated and dynamized using lactose as excipient, according to Brazilian Homeopathic Pharmacopoeia. Lactose samples (LAC 1–3c) were also prepared following the same protocol and used as controls. The samples were analyzed structurally by Atomic Absorption Spectroscopy (AAS), X-ray Diffraction (XRD), Transmission Electron Microscopy (TEM) with Energy Dispersive X-ray Spectroscopy (EDX) and Scanning Electron Microscopy (SEM), and thermodynamically by Thermogravimetry (TG) and Differential Scanning Calorimetry (DSC).

Results: AAS analysis detected 97.0 % of zinc in the raw material, 0.75 % (*Zinc met* 1c) and 0.02% (*Zinc met* 2c). XRD analysis showed that inter-atomic crystalline spacing of lactose was not modified by dynamization. Amorphous and crystalline lactose spheres and particles, respectively, were observed by TEM in all samples, with mean size from 200 to 800 nm. EDX obtained with TEM identified zinc presence throughout the amorphous matter but individualized zinc particles were not observed. SEM images obtained from dynamized samples (LAC 1c and *Zinc met* 1c) with electron backscattering could not identify zinc metal grains. The dynamization process induced Derivatives of Thermal Gravimetric (DTg) peak modification, which was previously centered near 158°C to lactose, to a range from 140 to 170°C, suggesting the dynamization process modifies the temperature range of water aggregation. Thermal phenomena were analyzed and

*Correspondence: Carla Holandino, Multidisciplinary Laboratory of Pharmaceutical Sciences and Laboratory of Research and Development of Integrative and Complementary Medicine, Department of Drugs and Medicines, Pharmacy College, UFRJ, Rio de Janeiro, Brazil.

E-mail: cholandino@gmail.com

Received 7 July 2016; revised 19 June 2017; accepted 21 June 2017

visualized by Analysis of Variance (ANOVA) and Principal Component Analysis (PCA) statistics. Both indicated that fusion enthalpy of dynamized samples (DynLAC 1-3c; DynZn 1-3c) increased 30.68 J/g in comparison to non-dynamized lactose (LAC; $p < 0.05$). **Conclusions:** Our results suggested no structural changes due to the trituration and dynamization process. However, TG and DSC analyses permit the differentiation of dynamized and non-dynamized groups, suggesting the dynamization process induced a significant increase in the degradation heat. These results call for further calorimetric studies with other homeopathic dilutions and other methodologies, to better understand the dynamics of these systems. *Homeopathy* (2017) **106**, 160–170.

Keywords: Physicochemical; Homeopathy; *Zincum metallicum*; Lactose; Trituration

Abbreviations: XRD, X-ray diffraction; TEM, transmission electron microscopy; EDS, energy dispersive X-ray spectroscopy; SEM, scanning electron microscopy; AAS, atomic absorption spectroscopy; TG, Thermogravimetry; DTg, derivatives of thermal gravimetric ANALYSIS curves; DSC, differential scanning calorimetry; SE detector, Secondary electrons detector; BSE, electron backscattered; PCA, principal component analysis

Introduction

Homeopathic medicines are prepared through processes of dilution and shaking or succussion (called “dynamization” or “potentization” in the homeopathic pharmacopoeia), using exact quantities of active ingredient mixing and inert excipient (lactose).¹ Early in the 19th century, a prior trituration process was credited with the ability to render even insoluble substances in soluble. Initially, plant extracts were not triturated. However, in 1835, Hahnemann concluded that all substances should be hand-triturated, to the 3c and 6× potencies.² In 1842, 3c trituration was also adopted as the required starting point for the manufacture of LM potencies.³

Since Hahnemann’s initial steps in the trituration process, its peculiar features were investigated by a number of experimental approaches, such as spectroscopic measurements and NMR analyses. Other approaches, including quantum physics and nanoscience,^{4–6} may increase our understanding of physicochemical properties of solid homeopathic medicines. Botha and Ross reported statistically significant differences in NMR chemical shifts, as well as relative integration values of some signals from triturated and non-triturated homeopathic samples.⁴

Some aspects of homeopathic drugs include speculative hypotheses such as the one proposed by Molski,⁵ in which potentization belongs to the class of quasi-quantum phenomena, playing an important role both in biological systems and homeopathy. Another such hypothesis identifies nanoparticles (NPs) at homeopathic solid dilutions, as reported by Chikramane *et al.*⁶ These authors demonstrated that the hydroxyl groups in lactose could interact with the metal particles by hydrogen bonds, as shown by specific infrared stretching/vibrational frequencies. Non-covalent interactions with lactose seem to stabilize metal particles, including formation of NPs.⁶

Also, it has been speculated that NPs can occur in homeopathic products as a result of trituration and subsequent shaking in glass containers.^{7,8} In fact, presence of nanostructures in homeopathic solutions were detected in highly diluted samples.^{7,8}

The physicochemical nature of homeopathic medicines is still far from being clarified, as too are the properties of NPs produced by the dynamization process. Some reports suggest changes in physicochemical properties, with potential biological implications of homeopathic dilutions.^{9–15} Further developments in basic research are highly desirable, and one important challenge will be the development of theoretical and experimental methods able to yield consistent and reproducible results.¹⁶

The need for a better understanding of dynamized systems motivated the *International Research Group on Very Low Dose and High Dilution Effects* (GIRI) to develop a multicentric project using a single metal, zinc, prepared by a unique laboratory (UFRJ, Rio de Janeiro, Brazil), following the same Pharmacopoeia (Brazilian Homeopathic Pharmacopoeia). Research on *Zincum metallicum* can make a valuable contribution, as shown in recent studies performed by GIRI’s researchers, with animal, wheat seed¹⁹ and physical models^{16,21} indicating that this initiative introduces new important knowledge about dynamized systems.

Zinc is an essential microelement required for various cellular functions, including cerebral depression,²² acting as antioxidant, structural constituent in numerous proteins, and participating in cognitive development, immune response, thymus activity, and others.^{23,24}

This paper aims to consider how traditional homeopathic manufacturing process modifies the physicochemical properties of *Zinc met*, comparing findings with dynamized and non-dynamized lactose. Then, different experimental tools were employed in order to characterize and increase the understanding of dynamized solid systems. This research is

under development as a formal Brazilian-Italian inter-university partnership.

Materials and methods

Samples and controls

Potencies were produced manually according to the Good Manufacturing Practices at the Faculty of Federal University of Rio de Janeiro, following the Brazilian Homeopathic Pharmacopoeia guidelines.¹ The starting materials, zinc and lactose monohydrate, were purchased from Labsynth Ltd. (Diadema, Brazil) and Pharma Nostra Comercial Ltda (Rio de Janeiro, Brazil), respectively. Zinc raw material (99.0 % of zinc, 0.01% of iron, as declared by the supplier) was acquired as crystalline bars and was manually scraped using a metallic spatula until it became a fine powder.

The homeopathic manufacturing process followed the statements of the Brazilian Homeopathic pharmacopoeia and started with the lactose separation, in three equal parts.¹ One third of the lactose was placed in porcelain vessel to avoid zinc loss. Following this, zinc was added and triturated, meeting the centesimal scale (1 part of material to 99 parts of inert vehicle), and the complex (*Zinc met* plus lactose) was submitted to two independent and vigorous cycles of crushing and scraping for 20 min. After this first cycle, the second and third parts of lactose were added to the porcelain vessel, and submitted to the second and third cycles of crushing and scraping, for 20 min each, respectively. The dynamization process was concluded at the end of 60 min.

Each sample received the designation of first triturated 1/100, coded as *Zinc met* 1c. For the second triturated compounding, 1 part of the first one (1c) was mixed in 99 parts of lactose (centesimal scale), and all crushing and scraping procedures were repeated to obtain *Zinc met* 2c¹. The last dynamization process produced *Zinc met* 3c, following the same protocol described above, using 1 part of *Zinc met* 2c for 99 parts of lactose. Control samples were prepared with dynamized lactose (LAC 1–3c) and non-dynamized lactose (LAC).

Zinc content by AAS

Content was determined by Atomic Absorption Spectroscopy (AAS) using a Shimadzu (AA-6800) Spectrophotometer operated with air-acetylene flame atomizer. The following samples: zinc (raw material), *Zinc met* 1c, *Zinc met* 2c, *Zinc met* 3c, and lactose (Table 1) were analyzed

according to two independent sets. A calibration curve was previously constructed and the absorbance values of respective analyses were compared to this calibration curve, allowing the calculation of atom content in each sample. Zinc absorbance was measured at 213.9 nm.

X-ray powder diffraction

About 50 mg of each sample (LAC 1 and 2c; *Zinc met* 1 and 2c; zinc grains; lactose) was analyzed in a PANalytical (Almelo, the Netherlands) X'Pert PRO diffractometer using CuK α radiation (λ 1.5418 Å). The X-ray powder diffraction (XRD) pattern was recorded from 10° to 50° with a step size of 0.02° and counting time of 5 sec/step. The position of peaks in the diffractograms (2θ) was used to determine the interplanar distances (d_{hkl}) following Bragg's law (where hkl refers to Miller indices):

$$2d_{hkl} \sin \theta = n\lambda$$

The d_{hkl} values were compared to standard powder diffraction data in the literature.²⁵

Scanning electron microscopy

Zinc met 1c and LAC 1c were affixed in aluminum stubs with a carbon tape, submitted to the critical point drying and gold coating, following scanning electron microscopy protocol. Samples were observed in JEOL JSM-7100F field emission SEM operated at 5 kV of accelerating voltage. The analyses were carried out at the Brazilian Center for Physics Research (CBPF, Rio de Janeiro, Brazil).

Scanning electron microscopy associated with X-ray microanalysis

Samples of *Zinc met* 1c and LAC 1c were dissolved in 5 mL at the concentration of 10 mg/mL of ultrapure water (centesimal dilution), and centrifuged to concentrate the particulate matter as described below. The solutions were mechanically succussed in a DynaA dynamizer (130 hits in 7 s) in soda-lime sterile tubes, transferred to plastic centrifuge tubes, and spun at 10,800 $\times g$ for 30 min at room temperature in a Beckman–Coulter Optima LE-80K ultracentrifuge. Visual inspection, after centrifugation, showed a dark pellet in *Zinc met* 1c and a clear white bottom in LAC 1c sample. The supernatants were carefully removed and the pellets recovered by the addition of 50 μ l pure water. *Zinc met* 1c and LAC 1c pellets (0.3 μ l-drops) were transferred to stubs with a plastic bottom, dried at 37°C for 1h, and examined with an XL30 ESEM scanning

Table 1 Concentration of zinc, potassium, iron, calcium and phosphorus measured by AAS analyses in weight percent (wt%)

| Sample | Concentration in weight percent (wt%) | | | | |
|----------------------------------|---------------------------------------|----------------|----------------|------------------|------------|
| | Zinc | Potassium | Iron | Calcium | Phosphorus |
| Zinc | 97.00 \pm 1.4 | 0.01 \pm 0.8 | 0.04 \pm 2.4 | ND | ND |
| <i>Zinc met</i> 1c (1/100) | 0.75 \pm 0.5 | 0.03 \pm 0.5 | ND | 0.0046 \pm 0.7 | ND |
| <i>Zinc met</i> 2c (1/10.000) | 0.02 \pm 2.2 | 0.03 \pm 0.5 | ND | 0.0044 \pm 0.4 | ND |
| <i>Zinc met</i> 3c (1/1.000.000) | ND | 0.03 \pm 0.4 | ND | 0.0040 \pm 0.4 | ND |
| Lactose | ND | 0.02 \pm 0.2 | ND | 0.0052 \pm 1.1 | ND |

ND: not detected.

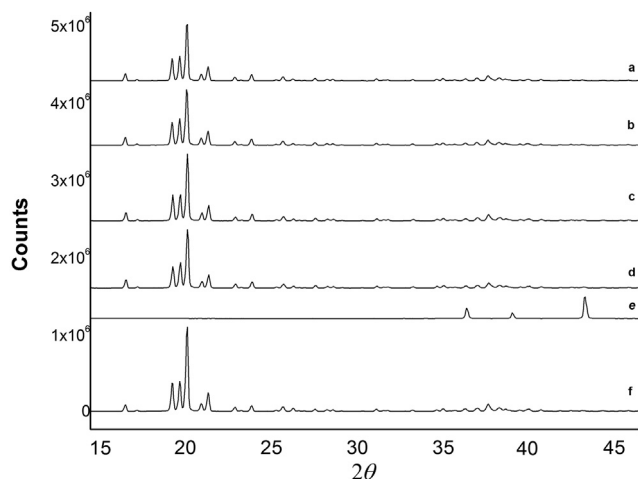


Figure 1 XRD patterns of dynamized and non-dynamized samples. (a) LAC 3c; (b) LAC 1c; (c) *Zinc met* 1c; (d) *Zinc met* 2c; (e) zinc; (f) Lactose.

Table 2 Interplanar distances (d_{hkl}) and relative intensity signal of peaks (Int %) obtained from XRD data of zinc, and non-dynamized lactose (Lactose) and dynamized lactose (LAC 1c, LAC 3c)

| Zinc | | Lactose | | LAC 1c | | LAC 3c | |
|-----------|-----|-----------|-----|-----------|-----|-----------|-----|
| d_{hkl} | Int | d_{hkl} | Int | d_{hkl} | Int | d_{hkl} | Int |
| 2,47 | 49 | 7,06 | 12 | 7,06 | 18 | 7,06 | 17 |
| 2,31 | 27 | 5,39 | 8 | 5,39 | 15 | 5,39 | 14 |
| 2,09 | 100 | 4,63 | 34 | 4,63 | 42 | 4,63 | 40 |
| 1,69 | 19 | 4,53 | 36 | 4,53 | 48 | 4,53 | 44 |
| 1,34 | 18 | 4,43 | 100 | 4,44 | 100 | 4,43 | 100 |
| 1,33 | 13 | 4,26 | 10 | 4,26 | 14 | 4,26 | 13 |
| | | 4,18 | 23 | 4,18 | 26 | 4,18 | 26 |
| | | 3,89 | 5 | 3,90 | 8 | 3,90 | 8 |
| | | 3,73 | 7 | 3,73 | 12 | 3,73 | 12 |

electron microscope under high vacuum (FEI Company, Eindhoven, Netherlands) equipped for Energy Dispersion Analysis of X-Ray (EDX). These analyses were carried out at the Technology Platform Center of the University of Verona (Italy).

Particle size estimation by optical microscopy

Zinc met 1c (15.5 mg), *Zinc met* 2c (85 mg) and LAC 1c control (15.5 mg) powders were dissolved in 1.5 ml of pure water, centrifuged in minifuge at 13,000 rpm for 30 min, suspended in 50 μ l of pure water, and observed in a Burkler chamber by contrast phase microscopy, using an Olympus IX50 microscope with 100 \times original magnification.

Transmission electron microscopy

Samples of lactose; LAC 1 and 3c; *Zinc met* 1 and 3c were prepared using alcohol 96%, at a concentration of 5.0 mg/mL. Afterward, 10 μ L of the solution was dropped on Formvar-coated TEM copper grids, air-dried, and observed in a JEOL 2100F operated at 200 kV equipped with an energy-dispersive X-ray spectroscopy (EDX) (Noran Seven).

Thermal analysis by differential scanning calorimetry (DSC) and thermogravimetry (TG)

DSC and TG analyses were performed on a Shimadzu DSC60 and Shimadzu TG50, respectively. The samples analyzed were: lactose; LAC 1 and 3c; *Zinc met* 1 and 3c. DSC was performed in duplicate. The conditions used for the DSC analysis were as follows: sample weight (1–3.4 mg), aluminum cell, flow rate (50 mL/min), temperature rate (10°C/min until 230°C) under N₂ atmosphere. An empty alumina cell was used as reference and the heat flow between the sample and reference pans was recorded.

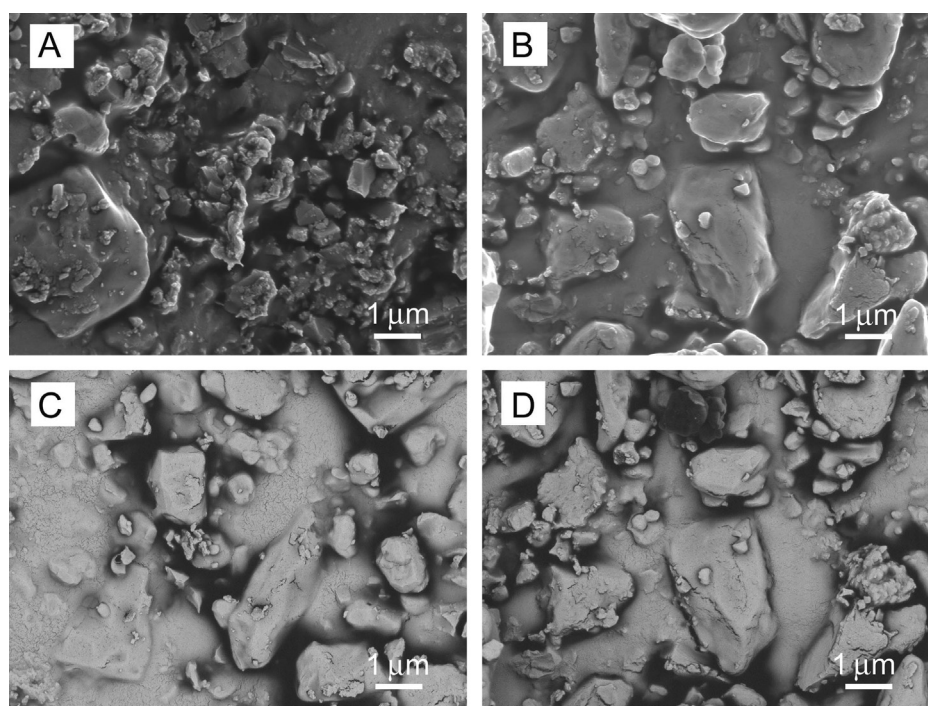


Figure 2 SEM obtained with SE (A and B) and BSE (C and D) detectors. A – LAC 1c. B – *Zinc met* 1c. C – LAC 1c. D – *Zinc met* 1c.

The conditions of TG analysis were: sample weight (± 5 mg), platinum cell, flow rate (50 mL/min), temperature rate ($10^{\circ}\text{C}/\text{min}$ until 500°C ; $50^{\circ}\text{C}/\text{min}$ until 800°C) and atmosphere (nitrogen). The analyses were made at the Pharmaceutical Technology Laboratory of the Federal University of Rio de Janeiro.^{26,27}

Statistical analysis

Statistically significant differences among experimental groups for the enthalpy fusion values (DSC analysis) were detected based on differences between the individual means determined using a non-parametric ANOVA followed by Tukey's post hoc test. The statistical analysis was performed using the software GraphPad Prism 5 (GraphPad Software Inc., La Jolla, USA) and the significance level (p-value) was set to 0.05. Principal components analysis (PCA) is a procedure for identifying a smaller number of uncorrelated variables, called "principal components", from a larger set of data. The goal of PCA is to explain the maximum amount of variance with the fewest number of principal components. PCA was performed with Statistica[®] software by plotting two principal components (PC1 and PC2) as a function of both dehydration and crystallization enthalpies.

Results

Zinc met measurement in dynamized samples

The Atomic Absorption Spectroscopy (AAS) is a sensitive analytical technique that measures down to parts per

billion of a gram ($\mu\text{g dm}^{-3}$). This analysis detected 97.0 % of zinc in the raw material, 0.75% (*Zinc met 1c*) and 0.02% (*Zinc met 2c*), showing zinc concentration decreased with dynamization (Table 1). Besides, considering our interest to characterize the presence of other metals in these samples, Potassium (K), Iron (Fe), Calcium (Ca), and Phosphorus (P) were also quantified in different percentage amounts (Table 1). Lactose used as trituration excipient presented a minimum quantity of potassium (0.02 %) and calcium (0.0052 %), probably as contaminant ingredient.

Crystalline structure and morphology

XRD analyses from pure lactose (Lactose), triturated lactose (LAC 1c; 3c) and triturated lactose containing zinc (*Zinc met 1c*; 3c) were similar (relative intensity and position of diffracted peaks), suggesting the dynamization process was not able to modify lactose crystallinity, even in the presence or in the absence of zinc atoms, at centesimal proportions. Besides, zinc peaks could not be observed in LAC 1c and LAC 3c diffractograms (Figure 1). The interplanar distances (d_{hkl}) and relative intensities of peaks (Int %) from zinc and lactose (non-dynamized and dynamized) measured in Figure 1 are in accordance with previous literature reports²⁸ (Table 2). These XRD results suggested no mutual interaction in these centesimal homeopathic preparations.

The morphology of LAC 1c and *Zinc met 1c* were analyzed by SEM (Figure 2A and B). Analyses with the backscattered detector (Figure 2C and D) showed images

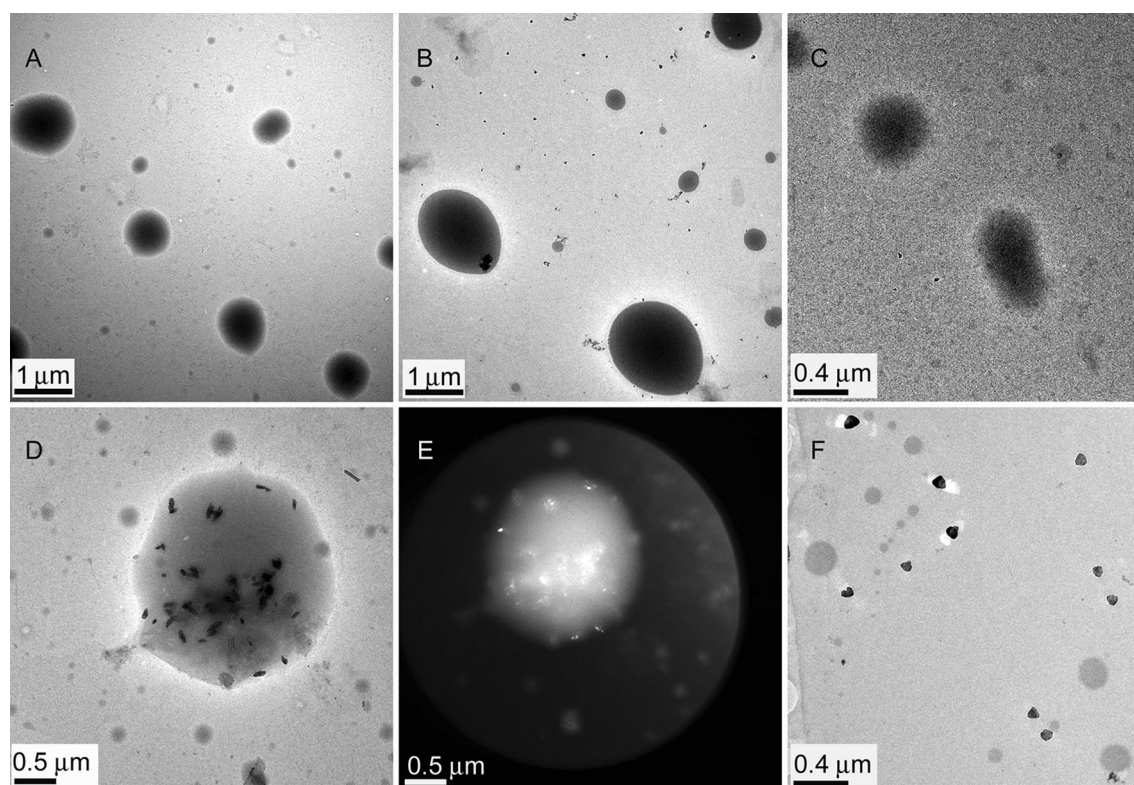


Figure 3 TEM ultrastructural analysis of lactose, *Zinc met 1c* and *Zinc met 3c* samples. A – Lactose; B – LAC 1c; C – LAC 3c; D, E – TEM bright and dark field analysis of *Zinc met 3c*; F – *Zinc met 1c*.

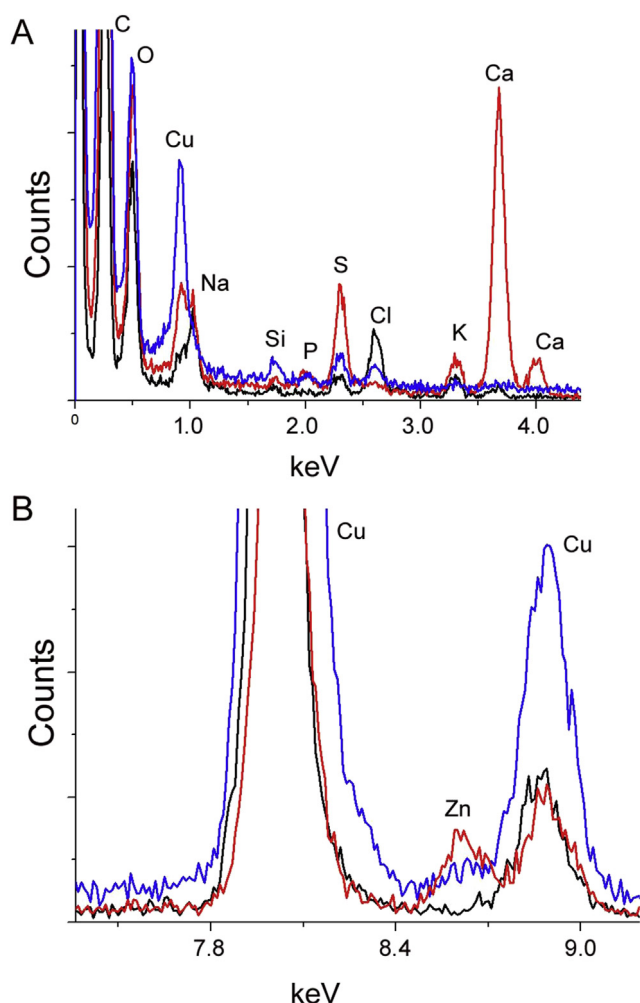


Figure 4 EDX obtained in the TEM of pure lactose samples; *Zinc met 1c* and *Zinc met 3c*. Black line: lactose; red line: *Zinc met 1c*; blue line: *Zinc met 3c*. A – Energy range from 0 to 4.0 KeV; B – Energy range from 7.0 to 9.0 KeV. (For interpretation of the references to color in this figure legend, the reader is referred to the web version of this article.)

with homogeneous contrast for both samples, indicating absence of large metallic zinc grains in *Zinc met 1c* sample at the observed magnification (Figure 2D).

Pure lactose, triturated lactose (LAC 1c and 3c), and *Zinc met* (*Zinc met 1c* and *Zinc met 3c*) samples were analyzed by TEM. Amorphous spheres from 200 to 800 nm were observed in all samples (Figure 3A–F). Crystalline materials were also detected in association with amorphous spheres or isolated from them, as seen by bright (Figure 3D) and dark (Figure 3E) fields, in which bright regions are indicative of crystallinity. However, individualized crystalline particles of lactose were also found outside spheres with similar morphology and dimension (Figure 3F). The presence of crystalline matter is in agreement with the XRD data which showed diffraction peaks of lactose in all samples (Figure 1). TEM results suggested no structural changes due to the dynamization process.

EDX compositional analyses (Figure 4A and B), obtained from pure lactose (black line), *Zinc met 1c* (red line), and *Zinc met 3c* (blue line), showed the presence of

low zinc amounts in some regions of *Zinc met 1c* and *Zinc met 3c* samples (Figure 4B). Sodium (Na), phosphorus (P), sulfur (S), chloride (Cl), potassium (K) and calcium (Ca) were also detected in all samples (Figure 4A). Copper (Cu) and siliceous (Si) x-rays are originated from the TEM grid and from the EDX detector, respectively.

Scanning electron microscopy and microanalysis in *Zinc met* solutions

SEM analysis of *Zinc met* samples performed in the laboratory of Verona University (Italy) confirmed the presence of zinc particles after extraction from *Zinc met 1c* solution. Since the molar presence of zinc versus lactose should be theoretically around 0.02% (2c; Table 1), it is likely that the failure of detection with EDX probe is due to technical limits, mainly in the ability to precisely locate a particle of zinc in the presence of a large excess of lactose particles. Therefore, in order to remove the lactose and to concentrate zinc particles, before the microscopic detection, *Zinc met 1c*, *Zinc met 2c* and LAC 1c samples were solubilized in pure water and submitted to high speed centrifugation. Then, *Zinc met 1c* showed a dark gray pellet, which was not present in lactose sample (*data not shown*). The structural analyses of *Zinc met 1c* pellets showed aggregates of smaller sub units, similar to a bunch of grapes (Figure 5A), and the microanalysis spectrum confirmed the zinc profile.

EDS analyses of *Zinc met 1c* pellet presented three characteristic zinc peaks due to the energy dispersion of the electrons produced in the various orbitals (about 1.0, 8.6, and 9.6 keV; Figure 5B and C). Zn was detected throughout the whole microscopic field (Figure 5B) at 15.33% molar weight and at higher level (27.48%) when focusing on a 0.5 μm -sized particle (Figure 5C). Control sample (LAC 1c) analyses showed the absence of zinc and the presence of carbon and oxygen peaks, both of them related to lactose itself and to the support surface (Figure 5D). *Zinc met 2c* pellet was obtained from a concentrate powder suspension (57 mg/mL).

The dimension of particulate matter in the pellet was estimated by optical microscopy on a micrometric grid slide and compared to the *Zinc met 1c* pellet (*data not shown*). *Zinc met 1c* showed particle sizes ranging from 10 to 40 μm while smaller particles (10–20 μm) were observed in *Zinc met 2c*. No particles were observed in LAC 1c sample (*data not shown*). Particles smaller than 10 μm cannot be visualized by this method.

Thermal analyses

Thermal properties were evaluated by both DSC and TG. The results suggest that both used thermal analyses are sensitive enough to identify aggregative differences between zinc and lactose. The first weight loss all the samples occurred between 120°C and 180°C: the peaked centered between 155°C and 165°C. This weight loss is commonly attributed to the loss of adsorbed water.²⁹ The trituration process induced DTg peak modification, which was previously centered near 158°C for lactose, to a range from 140

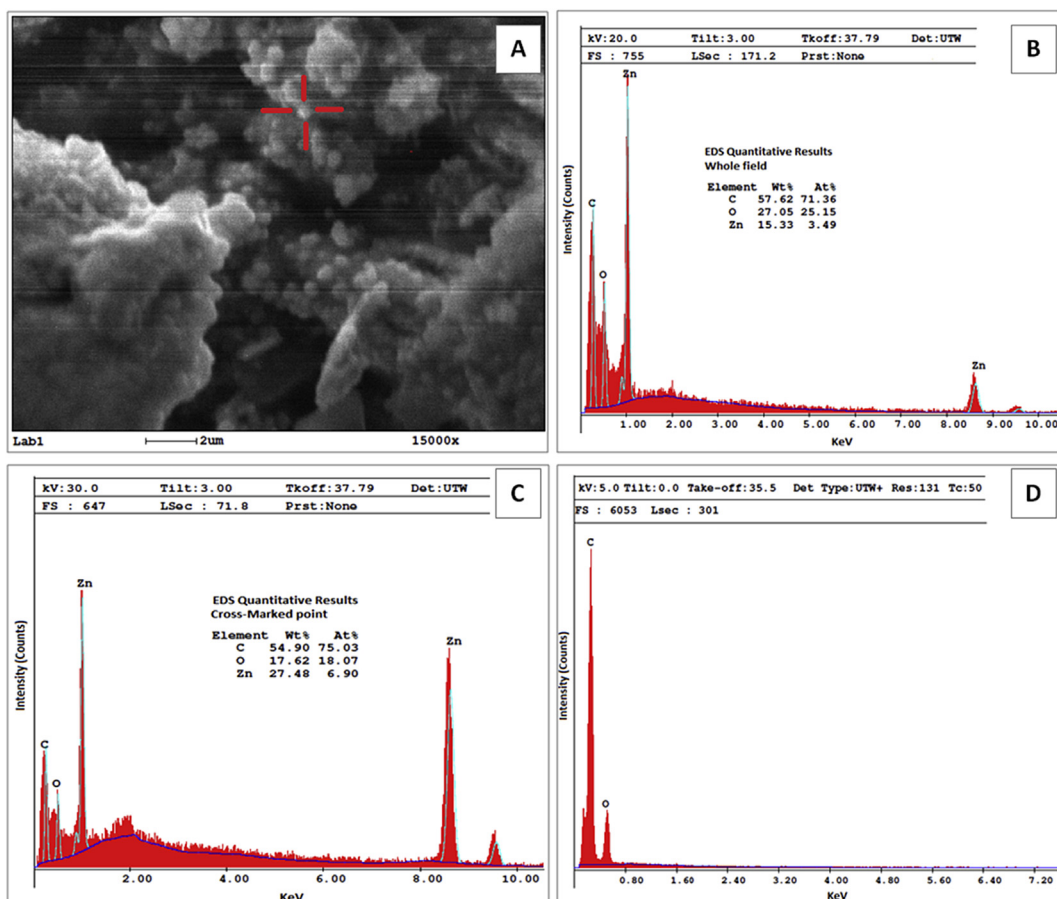


Figure 5 SEM image and microanalysis of the pellets from *Zinc met 1c* or LAC 1 solutions. A: SEM image at 15KX magnification of *Zinc met 1c* pellet; zoom on a metallic flake. B: *Zinc met 1c* microanalysis spectrum obtained by the EDAX (Energy Dispersion Analysis of X-Ray) probe and carried on the whole microscopic field. C: *Zinc met 1c* EDAX spectrum on cross-marked point of the image in panel A. D: EDAX spectrum of a drop of LAC 1c suspension.

to 170°C for all dynamized samples. Subsequent sample heating resulted in a continuous loss of weight. The second weight-loss peaks were around 260°C and were attributed to the melting of lactose crystals, followed by the last peak of lactose decomposition, around 322°C (Figure 6).

Figure 7 shows the comparison among DSC curves for all samples. DSC data showed an endothermic process near 145°C, which is attributed to a dehydration peak (Figure 7, white arrow) with enthalpy values ranging from 58.58 J/g to 77.01 J/g. The second endothermic process (Figure 7, black arrow) is near to 217°C and can be attributed to the crystalline fusion of lactose crystals with enthalpy values between 110.62 J/g and 173.58 J/g, as previously described by Figura and Epplé.³⁰

The effect of lactose dynamization on both dehydration (Figure 8A) and crystalline fusion (Figure 8B) enthalpies were better evaluated by ANOVA. Statistical studies indicated an increase of 30.68 J/g in fusion enthalpy when dynamized groups (DynLAC 1c-3c; DynZn 1c-3c) were compared to lactose (LAC; $p < 0.05$). No significant variation ($p > 0.05$) was observed in dehydration values as a function of process (Figure 8A). In order to elucidate this point, a subsequent statistical approach was applied to DSC results.

Principal component analysis (PCA) is one of the most popular multivariate statistical approaches used.³¹ In

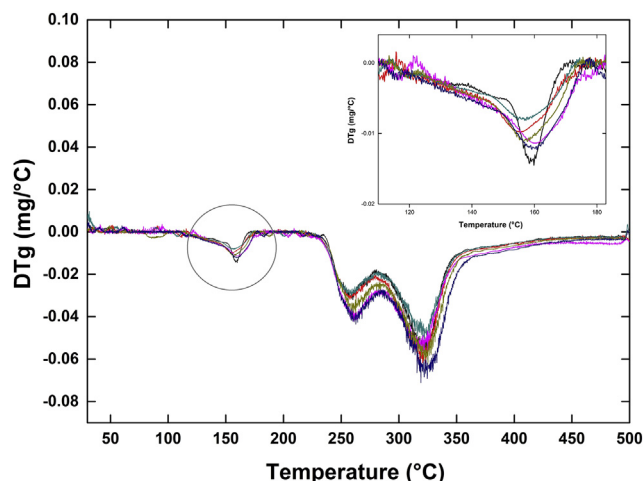


Figure 6 Derivatives of Thermal Gravimetric Analysis (DTg) curves of non-dynamized lactose (Lactose), dynamized lactose (LAC 1c–LAC 3c), and dynamized zinc (*Zinc met 1c*–3c) samples measured from 20 to 5000C with a heating rate of 10°C/min. Black line: lactose; red line: LAC 1c; blue line: LAC 2c; green line: LAC 3c; pink line: *Zinc met 1c*; yellow line: *Zinc met 3c*; dark blue line: *Zinc met 3c*. DTg curves of all samples in the range from 120°–180°C are shown on the upper right (plotted in set). (For interpretation of the references to color in this figure legend, the reader is referred to the web version of this article.)

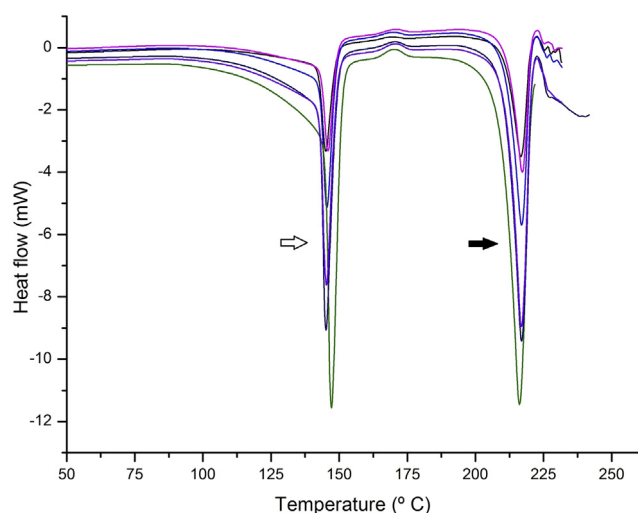


Figure 7 DSC curves of lactose control, dynamized lactose (LAC 1c–LAC 3c) and dynamized zinc samples (*Zinc met* 1c–3c) measured with a 10°C/min heating rate and flow rate of 50 ml/min. Black line: non-dynamized lactose (Lactose); red line: LAC 1c; blue line: LAC 2c; pink line: LAC 3c; green line: *Zinc met* 1c; dark blue line: *Zinc met* 3c; purple line: *Zinc met* 3c. White arrow shows the endothermic process, near 145°C, attributed to dehydration peaks; black arrow indicates the endothermic process of the crystalline fusion of lactose crystals. (For interpretation of the references to color in this figure legend, the reader is referred to the web version of this article.)

general, PCA analyzes a collection that represents different observations described by several dependent variables. In our case, all enthalpy values, in both dehydration and fusion processes, are collected as a function of sample composition (lactose and zinc) and dynamization, as showed in Table 3. PCA expresses a collection of data as a function of new orthogonal variables (principal components) that, in many cases, express a pattern of similarity among similar data. In the present paper, DSC enthalpy values are analyzed by PCA as projection of variables (loads) and of cases (scores) in factor planes. Figure 9A indicates that the factors (dynamization process) are perfectly positioned on the circle of correlations. The projection of variables (DynZn, LAC, DynLAC) on Factor 1 axis is similar, as shown in Figure 9A. On the other hand, the projection of these variables on Factor 2 axis indicates that these samples are statistically different. The projection of cases plot is presented in Figure 9B, and constructed using both dehydration and fusion enthalpy values obtained from DSC thermograms, as presented in Table 3 (see Supplementary data, Appendix A). The projection of all cases under Factor 1 × Factor 2 plane (98.77% correlation) shows two distinct data groups: one corresponding to dehydration values (right side), the other one (left side) to the crystalline fusion values (Figure 9B).

Discussion

Atomic absorption Spectroscopy (AAS) is a sensitive analytical technique that measures down to parts per billion of a gram ($\mu\text{g dm}^{-3}$). Here it showed that zinc

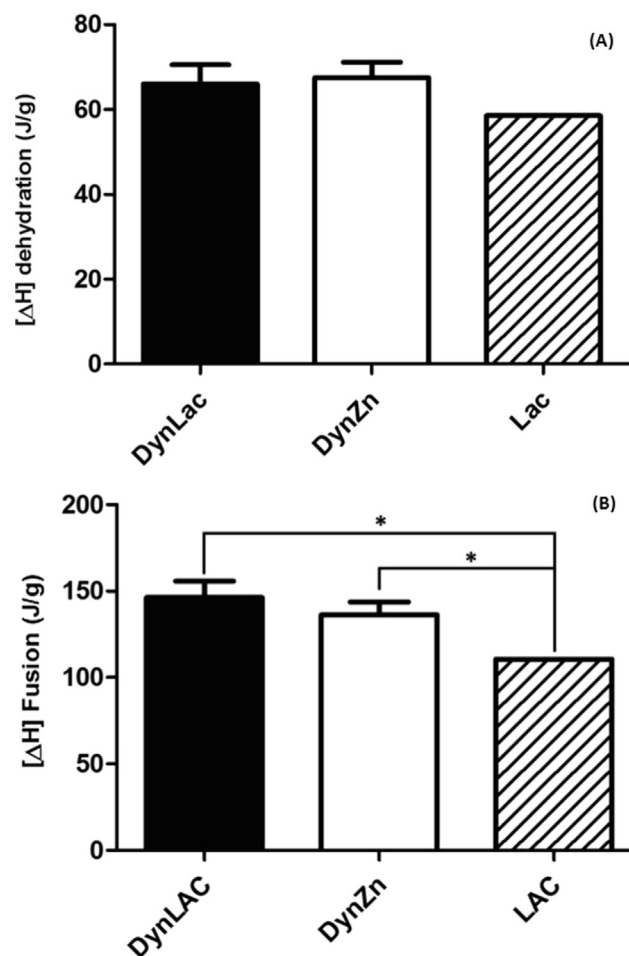


Figure 8 DSC data of the dynamized lactose group (DynLAC), the lactose control (LAC) and the *Zinc met* group (DynZn) by One-way ANOVA. A – Dehydration enthalpy; B – Fusion enthalpy; * $p < 0.005$.

Table 3 Dehydration and fusion enthalpy values obtained from DSC thermograms and used in PCA analyses

| $\Delta H(\text{J/g})$ | Samples | | | |
|------------------------|---------------|-----------------------------|--------------|--------|
| | Non-dynamized | Dynamized | | |
| | | LAC | Dynamization | DynLAC |
| Dehydration | 58.5 | 1c ^D | 68.75 | 52.34 |
| | | 2c ^D | 68.76 | 79.36 |
| | | 3c ^D | 45.85 | 68.92 |
| | | 1c ^{D_r} | 62.37 | 67.87 |
| | | 2c ^{D_r} | 77.01 | 64.26 |
| | | 3c ^{D_r} | 73.41 | 72.11 |
| Fusion | 110.62 | 1c ^F | 145.99 | 111.75 |
| | | 2c ^F | 150.43 | 157.69 |
| | | 3c ^F | 105.25 | 149.26 |
| | | 1c ^{F_r} | 141.66 | 127.76 |
| | | 2c ^{F_r} | 173.58 | 122.20 |
| | | 3c ^{F_r} | 160.74 | 149.27 |

c^D: dehydration value.
c^{D_r}: dehydration enthalpy value (duplicate).
c^F: fusion enthalpy value.
c^{F_r}: fusion enthalpy value (duplicate).
LAC: non-dynamized lactose.
DynLAC: Dynamized lactose samples (1–3c).
DynZn: *Zincum metallicum* samples (1–3c).

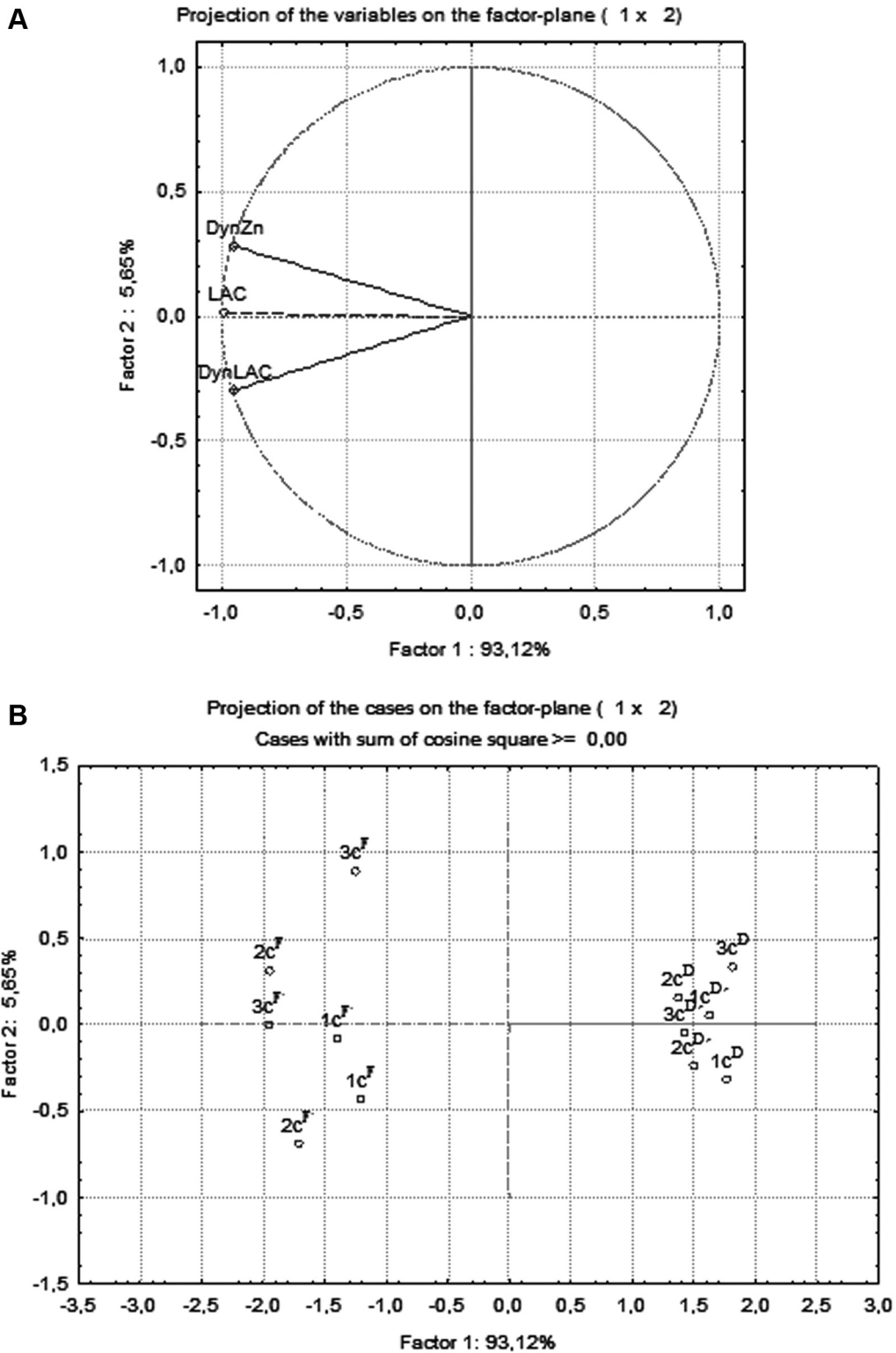


Figure 9 Fusion enthalpy of the dynamized lactose groups (DynLAC), the lactose control (LAC) and the dynamized *Zinc met* groups (DynZn) by PCA analysis. A – Projection of variables on the factor-plane (1X2) for lactose (LAC), dynamized lactose (DynLAC; 1–3c) and *Zinc met* (DynZn; 1–3c); B – Projection of cases on the factor-plane (1×2) for different dynamization processes (1c, 2c and 3c).

concentration decreases as the dilution process increases, as expected theoretically. The presence of other elements, such as calcium, potassium and iron, was also detected. Zinc, calcium and potassium were also identified by EDX.

The XRD pattern shows a typical crystalline material, with a high level of reflection overlap.³² Additionally, the dynamization process did not modify these diffraction patterns, regardless of the presence or absence of zinc atoms, in the centesimal samples analyzed. The *d*-spacing obtained from zinc and lactose were in agreement with XRD patterns described by Wyckoff²⁸ and Garnier *et al.*,³³ respectively. In order to confirm these results, it is important to analyze additional zinc mixtures, especially in higher zinc proportions. In fact, previous assays done by our group (Holandino *et al.*, unpublished results) in decimal proportion permitted us to register some zinc signals, even in 10⁻⁶ (6×; *data not shown*), indicating that further XRD experiments should be important to analyze mutual physical interactions between zinc and lactose in decimal homeopathic mixtures.

Scanning electron microscopy (SEM) analyses did not identify zinc grains in LAC 1c and *Zinc met* 1c samples, and no modification was observed by SEM micrographs in the lactose morphology after trituration. Given that SEM analyses use small amounts of samples, further experiments with different batches and homeopathic proportions could be helpful to better understand interactions between lactose and zinc.

Lactose monohydrate presents both crystalline and amorphous phases. TEM images showed crystalline and amorphous lactose particles with different morphologies and dimensions (200–800 nm). Crystalline materials were detected either in association with amorphous spheres or isolated from them, as detected in bright (Figure 3D) and dark (Figure 3E) fields (the bright regions are indicative of crystallinity). Some authors^{6,7} could detect the presence of nanoparticles of zinc, gold, tin, copper, even in extreme homeopathic dilutions, but results did not conclusively show the presence of zinc nanoparticles in a *Zinc 1c* sample. Although Zn signal was detected by EDX, no specific morphology could be associated with it, suggesting that zinc nanoparticles could be homogeneously dispersed throughout the lactose sample.

The presence of *Zinc met* pellets in 1c and 2c samples was observed in SEM and optical microscopy. They clearly showed that a considerable part of zinc grains remain insoluble in water, especially at first centesimal dilution (Figure 5). The optical microscopy analysis of *Zinc met* 1c compared to *Zinc met* 2c pellet suggested that the trituration process was efficient enough to decrease grain size, since trituration is a procedure to reduce particle dimension.

Differential scanning calorimetry (DSC) and thermogravimetry (TG) are techniques that can be used to identify molecular interactions and incompatibilities between drugs and excipients.^{34–36} These techniques are frequently used for rapid evaluations of physicochemical interactions^{37,38} using small sample sizes.³⁹ DSC experiments give information about enthalpy variation (ΔH),

change in specific heat, temperature peaks, as well as appearance, disappearance or shifts of exothermic or endothermic event peaks.^{38–40} On the other hand, TG analysis provides quantitative information about mass loss related to decomposition, evaporation or melting as a function of temperature.⁴¹

Thermal analysis of all dynamized samples showed different temperature ranges of water crystallization at DTg curves when compared to lactose, which could be attributed to the separation of lactose constituents induced by the trituration process. With the help of statistical tools, one may conclude that dynamization plays a significant role in the crystalline fusion of lactose (Figure 8B). Principal Component Analysis (PCA) of DSC data revealed the presence of three distinct groups (DynLAC; DynZn; LAC), indicating the dynamization process and the presence of zinc affect the position of fusion enthalpy values on principal component axes, in agreement with Konar *et al.*⁴²

The differences detected in fusion enthalpy values could be correlated with changes in samples' crystallinity, and consequently in their solubility. These results should motivate further studies with other dilutions and additional sensitive methodologies, such as NMR and Raman spectroscopy, in order to better understand the dynamics of these systems. The influence of these alterations on zinc solubility would be an additional important aspect to new investigations. Data obtained in this study may prove helpful for future research models in this field.

Conclusion

The present paper aimed to characterize physicochemical properties of homeopathic centesimal solid samples, prepared with zinc and lactose, according to Brazilian Homeopathic Pharmacopeia methodology. Our results suggested no structural changes due to the trituration process. Nevertheless, thermal analyses permit the differentiation of dynamized and non-dynamized groups suggesting the dynamization process was able to induce a significant increase in the degradation heat. Besides, by using principal component analysis as a statistical tool, it is possible to suggest the presence of zinc affects the position of fusion enthalpy values, which may be correlated with changes in sample crystallinity and consequent solubility. We hope that this multicentre project developed by GIRI will motivate new contributions to the development of homeopathic science.

Conflict of interest

No conflicts of interest exist.

Acknowledgements

The authors thank Prof Dr Silvana Marques Araújo and her research team (Maringá State University, Paraná, Brazil) for providing zinc (raw material) used in the present project. This work received funding from Brazilian Governmental Agencies (Fundação Carlos Chagas Filho

de Amparo à Pesquisa do Estado do Rio de Janeiro – FAPERJ and Conselho Nacional de Desenvolvimento Científico e Tecnológico – CNPq).

Supplementary data

Supplementary data related to this article can be found at <http://dx.doi.org/10.1016/j.homp.2017.06.003>.

References

- 1 Brazilian Homeopathic Pharmacopoeia. 3rd edn. Brazil: Ministerio da Saúde, 2011, p. 34.
- 2 Dellmour F. Importance of the 3c trituration in the manufacture of homeopathic medicines. *Br Homeopath J* 1994; **83**: 8–13.
- 3 Barthel P, Broese R, Cullen W, et al. Hahnemann's legacy – the Q (LM) potencies. *Br Homeopath J* 1991; **80**: 112–121.
- 4 Botha I, Ross AHA. A nuclear magnetic resonance spectroscopy comparison of 3C trituration derived and 4C trituration derived remedies. *Homeopathy* 2008; **97**: 196–201.
- 5 Molski M. Quasi-quantum model of potentization. *Homeopathy* 2011; **100**: 259–263.
- 6 Chikramane PS, Kalita D, Suresh AK, Kane SG, Bellare JR. Why extreme dilutions reach non-zero asymptotes: a nanoparticulate hypothesis based on froth flotation. *Langmuir* 2012; **28**: 15864–15875.
- 7 Chikramane PS, Suresh AK, Bellare JR, Kane SG. Extreme homeopathic dilutions retain starting materials: a nanoparticulate perspective. *Homeopathy* 2010; **99**: 231–242.
- 8 Bell IR, Schwartz GE. Enhancement of adaptive biological effects by nanotechnology preparation methods in homeopathic medicines. *Homeopathy* 2015; **104**: 123–138.
- 9 Holandino C, Leal FD, de Oliveira Barcellos B, et al. *Mechanical Versus Handmade Succussions: A Physical Chemistry Comparison. Signals and Images*. 2nd edn. Springer, 2008, pp 37–48.
- 10 Elia V, Baiano S, Duro I, Napoli E, Niccoli M, Nonatelli L. Permanent physico-chemical properties of extremely diluted aqueous solutions of homeopathic medicines. *Homeopathy* 2004; **93**: 144–150.
- 11 Elia V, Napoli E, Germano R. The “Memory of Water”: an almost deciphered enigma. Dissipative structures in extremely dilute aqueous solutions. *Homeopathy* 2007; **96**: 163–169.
- 12 Holandino C, Veiga VF da, Garcia S, Zacharias CR. Modeling physical-chemical properties of high dilutions: an electrical conductivity study. *Int J High Dil Res* 2008; **7**: 165–173.
- 13 Chaplin MF. The memory of water: an overview. *Homeopathy* 2007; **96**: 143–150.
- 14 Demangeat J-L, Gries P, Poitevin B, et al. Low-field NMR water proton longitudinal relaxation in ultrahighly diluted aqueous solutions of silica-lactose prepared in glass material for pharmaceutical use. *Appl Magn Reson* 2004; **26**: 465–481.
- 15 Wolf U, Wolf M, Heusser P, Thurneysen A, Baumgartner S. Homeopathic preparations of quartz, sulfur and copper sulfate assessed by UV-spectroscopy. *Evid Based Complement Altern Med* 2011; **1692798**.
- 16 Bellavite P, Marzotto M, Oliosio D, Moratti E, Conforti A. High-dilution effects revisited. 1. Physicochemical aspects. *Homeopathy* 2014; **103**: 4–21.
- 17 Silva SLM, Paula C, Soares LR, et al. Behavioral parameters evaluation after homeopathic Zincum metallicum treatment: a transgenerational study in mice. *Int J High Dilution Res* 2014; **13**: 47.
- 18 Ciupa L, Veiga FK, Portocarrero AR, et al. Zincum metallicum highly diluted and *Trypanosoma cruzi* mice infection: a protocol to evaluation. *Int J High Dilution Res* 2013; **12**: 143–145.
- 19 Kokornaczyk MO, Baumgartner S, Betti L, et al. Polycrystalline structures formed in evaporating droplets as a parameter to test the action of Zincum metallicum 30c in a wheat seed model. *Homeopathy* 2016; **105**: 173–179.
- 20 Ciupa L, da Veiga FK, Portocarrero AR, et al. Zincum metallicum 5cH increases survival and improves clinical mice infected with *Trypanosoma cruzi*. *Int J High Dilution Res* 2014; **13**: 111–113.
- 21 Marzotto M, Bonafini C, Debora O, et al. Detection of nanostructures in solutions of Zincum metallicum and the vehicle lactose. *Int J High Dilution Res* 2015; **14**: 41–44.
- 22 Vijnovsky B. *Tratado de Matéria Médica Homeopática*. Buenos Aires: Mukunda Publisher, 1980, p. 2028.
- 23 Fukada T, Yamasaki S, Nishida K, Murakami M, Hirano T. Zinc homeostasis and signaling in health and diseases: Zinc signaling. *J Biol Inorg Chem* 2011; **16**: 1123–1134.
- 24 Terrin G, Berni Canani R, Di Chiara M, et al. Zinc in early life: a key element in the fetus and preterm neonate. *Nutrients* 2015; **7**: 10427–10446.
- 25 Querido W, Abraçado LG, Rossi AL, et al. Ultrastructural and mineral phase characterization of the bone-like matrix assembled in F-OST osteoblast cultures. *Calcif Tissue Int* 2011; **89**: 358–371.
- 26 Abreu LCL, Todaro V, Sathler PC, et al. Development and characterization of nisin nanoparticles as potential alternative for the recurrent vaginal candidiasis treatment. *AAPS PharmSciTech* 2016; **17**: 1421–1427.
- 27 Villça JC, Silva LCRP, Barbosa LHF, et al. Preparation and characterization of polymer/layered silicate pharmaceutical nanobiomaterials using high clay load exfoliation processes. *J Ind Eng Chem* 2014; **20**: 4094–4101.
- 28 Wyckoff RWG. *Crystal Structures I*. 2nd edn. New York: Interscience Publishers, 1963, pp 7–83.
- 29 Listiohadi Y, Hourigan JA, Sleigh RW, Steele RJ. Thermal analysis of amorphous lactose and α -lactose monohydrate. *Dairy Sci Technol* 2009; **89**: 43–67.
- 30 Figura LO, Epple M. Anhydrous α -lactose a study with DSC and TXRD. *J Therm Anal* 1995; **44**: 45–53.
- 31 Abdi H, Williams LJ. Principal component analysis. *Wiley Interdiscip Rev Comput Stat* 2010; **2**: 433–459.
- 32 Kirk JH, Dann SE, Blatchford CG. Lactose: a definitive guide to polymorph determination. *Int J Pharm* 2007; **334**: 103–114.
- 33 Garnier S, Petit S, Coquerel G. Dehydration mechanism and crystallisation behaviour of lactose. *J Therm Anal Calorim* 2002; **68**: 489–502.
- 34 Thomas VH, Naath M. Design and utilization of the drug–excipient chemical compatibility automated system. *Int J Pharm* 2008; **359**: 150–157.
- 35 Monajjemzadeh F, Hassanzadeh D, Valizadeh H, et al. Compatibility studies of acyclovir and lactose in physical mixtures and commercial tablets. *Eur J Pharm Biopharm* 2009; **73**: 404–413.
- 36 Matos APS, Costa JS, Boniatti J, et al. Compatibility study between diazepam and tablet excipients. *J Therm Anal Calorim* 2017; **127**: 1675–1682.
- 37 Chadha R, Bhandari S. Drug–excipient compatibility screening – role of thermoanalytical and spectroscopic techniques. *J Pharm Biomed Anal* 2014; **87**: 82–97.
- 38 Maswadeh HM. Incompatibility study of ibuprofen in ternary interactive mixture by using differential scanning calorimetry. *J Therm Anal Calorim* 2016; **123**: 1963–1971.
- 39 Shantikumar S, Sreekanth G, SurendraNath KV, JaferValli S, Satheeshkumar N. Compatibility study between sitagliptin and pharmaceutical excipients used in solid dosage forms. *J Therm Anal Calorim* 2014; **115**: 2423–2428.
- 40 Botha SA, Lötter AP. Compatibility study between oxprenolol hydrochloride, temazepam and tablet excipients using differential scanning calorimetry. *Drug Dev Ind Pharm* 1990; **16**: 331–345.
- 41 Zayed MA, Fahmey MA, Hawash MF. Investigation of diazepam drug using thermal analyses, mass spectrometry and semi-empirical MO calculation. *Spectrochim Acta Part A Mol Biomol Spectrosc* 2005; **61**: 799–805.
- 42 Konar A, Sarkar T, Sukul NC, Sohel A, Sengupta A. Drugs at ultra high dilution induce changes in enthalpy associated with the loss of water of crystallization in lactose. *Environ Ecol* 2017; **35**: 554–557.